Including Experimental Aging of Shielded Cables into Bulk Current Injection Simulations

Oskari Leppäaho
Valeo
Créteil, France
oskari.leppaaho@valeo.com

Frédéric Lafon
Valeo
Créteil, France

Bruno Ferreri
Valeo
Créteil, France

Priscila Fernandez-Lopez
Valeo
Créteil, France

Marine Stojanovic
Valeo
Créteil, France

Richard Perdriau
Department of Electrical and Electronics Engineering
ESEO
Angers, France

Mohammed Ramdani
Department of Electrical and Electronics Engineering
ESEO
Angers, France

***Abstract*—Transfer impedance of shielded cables is a main characteristic to describe cable shielding performance at least up to 1 GHz. Traditionally, a cable shield consists of a braid, a foil, or a combination of them. Braids have attracted a significant amount of research interest, while foils have not. Published studies have concentrated on cable shielding performance when cables are new. In this paper, a highly accelerated aging method for shielded cables is presented and applied to a cable made up of a combination of a braid and foil shield. Finally, the effect of aging on system performance during bulk current injection (BCI) tests is assessed by circuit simulation.**

***Index Terms*—Electromagnetic compatibility, cable shielding, transfer impedance, aging, reliability, bulk current injection, simulation.**

I. Introduction

As automotive electrification and digitalization progress, shielded cables become increasingly important, on the one hand to convey information and to protect it from external disturbances, and on the other hand to confine the disturbance signals generated by electric drivetrains. When conveying information, a shielded cable often connects a sensor to an electronic control unit (ECU). This case will serve as an example in this paper. To provide proof of proper functioning of their product, automotive equipment suppliers use different electromagnetic compatibility (EMC) tests. One of them is bulk current injection (BCI) [1] that emulates the radio frequency (RF) field coupling to the equipment under test (EUT) through the cables connected to it. This paper aims to show, by simulation, how the BCI test result can be affected by aging of a shielded cable i.e. if more RF field is coupled to the EUT after the cable has aged.

To characterize the shielding performance of a shielded cable, two competing definitions are generally used: shielding effectiveness (SE) and transfer impedance (Z_T) [2]. SE is more a system property, whereas transfer impedance can be used in a circuit-like analysis. Our aim is to use SPICE-compatible modeling language and, thus, transfer impedance is a natural choice for the shielding performance metric. The most prominent ways to measure transfer impedance below 1 GHz are line-injection and triaxial methods [3], whereas other methods, such as reverberation chambers can be used above 1 GHz [4]. As the maximum frequency of the BCI test is limited to 400 MHz, one of the low frequency methods needs to be selected. Due to mechanical robustness reasons we selected the triaxial method, which is described in Section II-A.

Thermal [5] and mechanical [6] stress tests of automotive assemblies are well known. However, EMC testing during or after environmental stress of the full system presents an added cost, which is often considered excessive. Instead, subassemblies like EM interference (EMI) filters have been tested and characterized [7]. To this date, publications about aging of shielded cables have focused on testing of the cable dielectric performance parameters like insulation breakdown voltage and relative permittivity [8]. In this paper, the focus is on the shielding performance deterioration during thermal and mechanical stress. An overview of a newly developed triaxial cell for environmental testing, and the aging cycle used with it, are presented in Section II. Then, our first results of shielding performance aging are presented in Section III. Additionally, a simple model to consider aging during design process is presented. This model is based on a simple transfer impedance equivalent circuit [9] and used in the BCI compliance analysis in Section IV.

II. Aging and measurement method

This section briefly describes the used methodology. For the parts of the methodology, which have not been previously verified in literature, a brief verification against state-of-the-art is presented. The triaxial cell to measure transfer impedance is described in Section II-A, and the accelerated life condtions, which both the triaxial cell and the cable sample inside it are subjected to, are described in Section II-B.

978-1-7281-5579-1/20/$31.00 ©2022 IEEE

A. Triaxial cell

To perform the highly-accelerated thermal and mechanical stress tests of a shielded cable, we developed a hexagonal triaxial cell shown in Fig. 1 installed in the test chamber. The cell was developed so that it could be mounted in a highly accelerated life test (HALT) chamber, and that it would withstand the stresses imposed to it during testing. Before conducting the tests, the cell performance on transfer impedance measurement of the studied shielded cables was compared to a commercial cell with good equivalence of the measurement results as shown in Fig. 2. However, two concerns need to be addressed in those results:

1) Between 2 and 200 MHz our triaxial cell shows significantly lower transfer impedance and an additional plateau. This is likely due to torsion experienced by the cable, when it was mounted into the cell. It will be shown in Section III that this torsion is relaxed during the tests.
2) This cable provides low transfer inductance compared to its transfer resistance. Thus, the transfer inductance value needs to be deduced from the portion between 100 MHz and 1 GHz, where neither the cable sample nor the triaxial cell are electrically short. In the commercial cell, the sample length was 30 cm and, in our cell, it was 25 cm. Thus, the resonance points do not match. Moreover, there seems to be significant ($\sim$ 6 dB) sample-to-sample variation in the measured transfer inductance that is deduced from the peaks of the anti-resonance points. Resonances could be compensated by using a de-embedding method developed for triaxial cells [10] yielding to a better approximation of the transfer inductance. However, the de-embedding process needs additional measurements, like time-domain reflectometry (TDR), that were not performed during our aging tests. The inductance deduced from the measurement in our cell seems to correspond to the worst case and is accurate enough for the analysis presented in this paper.

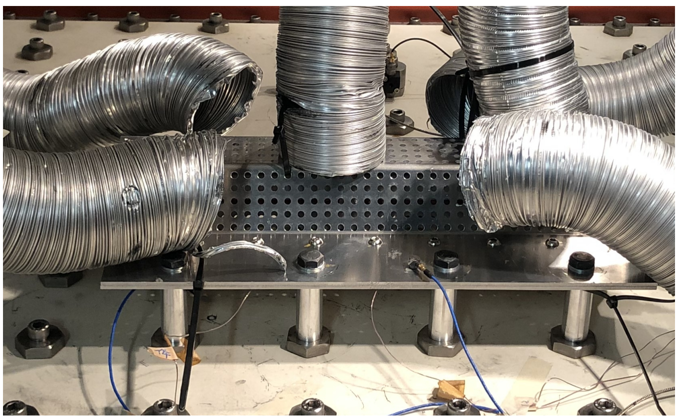

Fig. 1. Triaxial cell in HALT chamber with air guides to accelerate thermal transients.

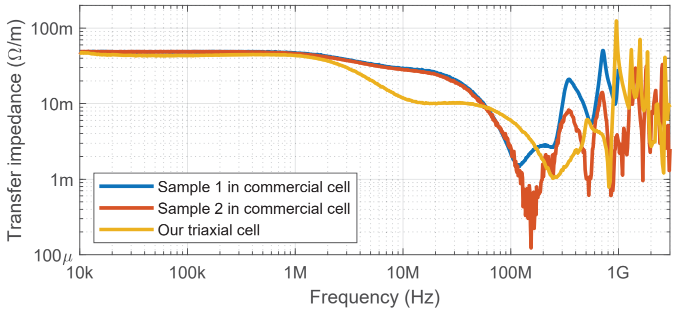

Fig. 2. Comparison of a commercial triaxial cell results to our cell results with fresh cable samples.

B. Highly Accelerated Life Testing (HALT)

The HALT test cycle coarsely follows an automotive original equipment manufacturer (OEM) standard [11] and includes four separate sections, as shown in Fig. 3:

A) Thermal step test with 5-minute dwell-time and 10°C steps over the cable's operating temperature range
B) Thermal transient stress test with setpoints at minimum and maximum operating temperatures of the cable and 5-minute dwell-time at each extreme
C) Vibration step test with 5-minute dwell-time and $10g_{rms}$ steps up to the maximum vibration level allowed by the test system
D) A maximal stress test with features from B and C combined and vibration dwell-time increased to ten minutes to enable a complete thermal cycle

To ensure the best possible transfer impedance measurement, no temperature or acceleration sensors were mounted inside the triaxial cell. The temperature of the triaxial cell was measured at the end of the cell. Based on our previous tests, it was observed that cable jacket temperature followed inlet air temperature with a 1-minute time-constant due to thermal inertia. This time constant was used in Fig. 3 to estimate jacket temperature based on inlet air temperature measurement. During thermal cycling at maximum temperature, the estimated jacket temperature overshot the setpoint by 10°C while the triaxial cell remained below setpoint by a similar amount. At minimum temperature, the estimated jacket temperature reached the setpoint, but the cell structure remained 20°C warmer. As can be seen from section A in Fig. 3 (top), with smaller temperature steps, no such differences exist. Thus, this effect can be considered as a characteristic of the test system. It could be compensated by reducing the mass of the triaxial cell, but that could reduce the vibration immunity of the setup.

As far as vibration was concerned, only table acceleration was measured with a sensor integrated in the chamber, and the triaxial cell was considered to represent typical mounting of the cable with 25 cm tying interval. At 70 and $80g_{rms}$, the sensor saturated on some of the highest vibration peaks. This phenomenon was not expected, and later troubleshooting with the chamber manufacturer revealed a sensor configuration error. Due to this configuration error, measurements at 70 and

$80g_{rms}$ setpoints show underestimated values.

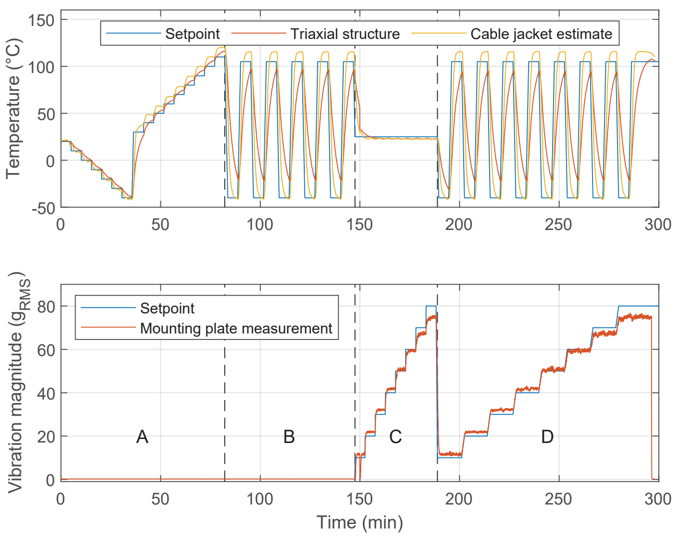

Fig. 3. HALT test cycle with thermal and vibration stress divided into four sections A-D.

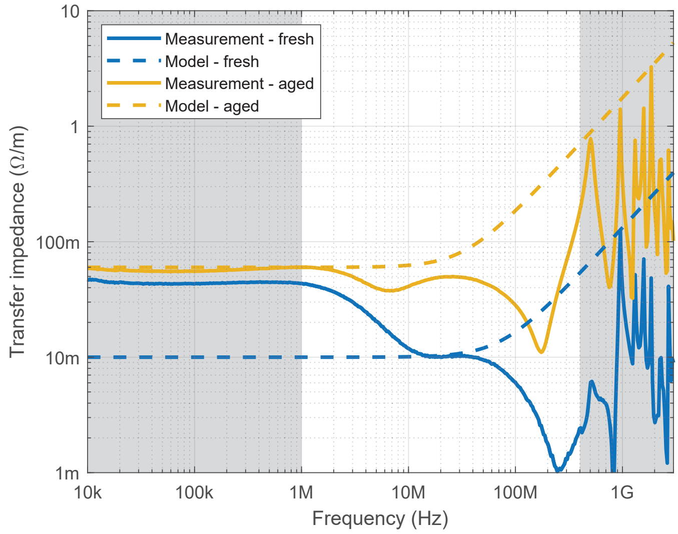

Fig. 4. Transfer impedance measurement results and models for a fresh and an aged cable.

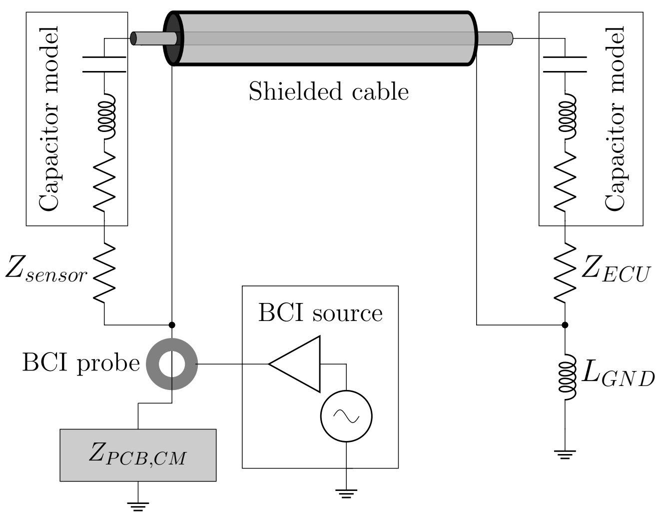

Fig. 5. BCI test simulation schematic

III. Aging Results and Modeling

As mentioned in Section II, the transfer impedance of a braid and foil shielded coaxial cable was measured in laboratory ambient conditions. Then, the cable sample was aged with the method presented in Section II, and its transfer impedance was measured again once the sample reached back to stable laboratory ambient conditions. Then, a simplified transfer impedance model [9]

$$Z_T = R_T + j\omega L_T \tag{1}$$

with transfer resistance (R_T) and transfer inductance (L_T) was fitted to the results as shown in Fig. 4. The regions between 10 kHz and 1 MHz as well as between 400 MHz and 3 GHz are not relevant for the BCI simulation, but are shown for completeness. The model parameters used are gathered in Table I.

TABLE I
Transfer Impedance Model Parameters

Parameter	New	Aged
R_T	10 mΩ/m	60 mΩ/m
L_T	21 pH/m	280 pH/m

Here, a best/worst-case modeling approach was taken to highlight the worst possible aging with a single sample. It means that for the fresh sample the lowest practicable transfer resistance and inductance were taken, whereas for the aged sample, highest practicable values were taken. As the fresh sample had two distinct resistance levels, the lower one around 20 MHz was selected. For the aged sample, the highest resistance around 1 MHz was selected. For transfer inductance, no steady measurement level with 20 dB/decade slope exists. The best inductance approximation can be achieved by matching it to the highest anti-resonance peaks before they turn into constant envelope [12]. By testing just one sample, this method captures most of the conditions that the designers need to foresee. In addition, the used model is simple compared to the real behavior of the cable that has both foil and braid shields. However, for system level modeling in the concept phase of product development, the chosen approach is accurate enough.

IV. BCI Simulation

To highlight the effect of cable shield aging on a practical electronics design, a generic automotive sensor connected to an ECU is taken as an example. A simple concept-level simulation circuit shown in Fig. 5 is used. It is formed by following an established simulation schematic [13] and consists of two integrated circuits (ICs) communicating with each other. In the concept phase, it is assumed that the IC selection is not yet firm

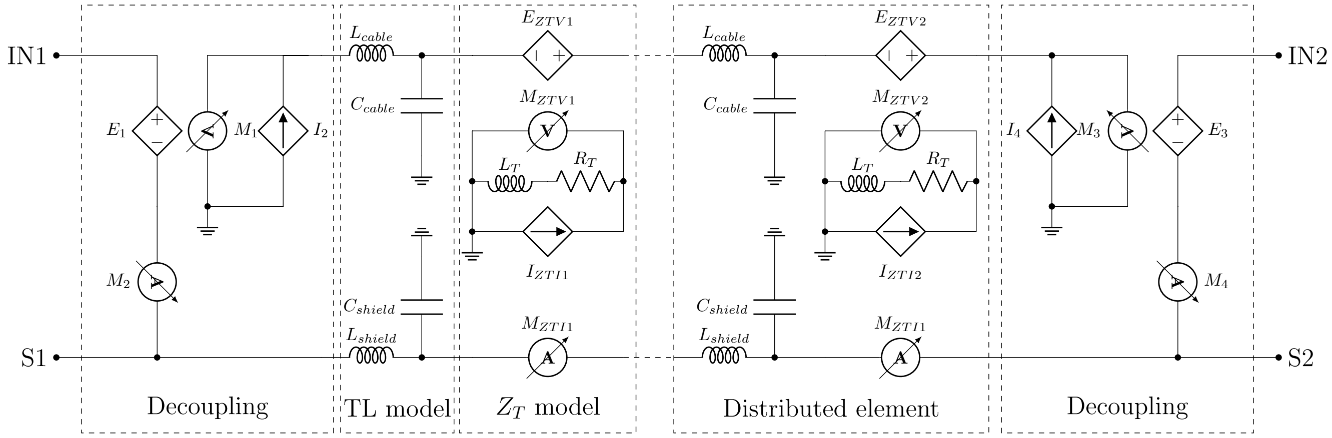

Fig. 6. Schematic of the shielded cable model. IN1 and IN2 are the inner conductor terminals and S1 and S2 are the respective shield ends.

and, thus, both are modeled as a 50-ohm impedance (Z_{sensor} & Z_{ECU}) with an immunity level of 50 mV over the tested frequency band of 1 to 400 MHz. This model is a simplified version of an IC immunity model introduced in [13]. The ICs communicate through a capacitively coupled transmission line using the shielded cable, which is our study target. The sensor IC is mounted on a printed circuit board (PCB), which has parasitic common mode (CM) impedance ($Z_{PCB,CM}$) to ground modeled as an RLC-circuit [13]. The ECU side is grounded to the vehicle chassis with a wire that is modeled as an inductance (L_{GND}).

As mentioned in [14], cable and injection probe models can be separated. The modeling of the injection probe together with the related signal source and amplifier is carried out as described in [13] with the source amplitude set according to a randomly selected OEM specification. For the shielded cable, the model shown in Fig. 6 is used. As can be seen from the system schematic in Fig. 5, neither end of the cable shield is connected to the system ground. In this scenario, it becomes paramount to ensure that no signal leakage from the center conductor to the system ground happens at the model level. Thus, decoupling circuits are introduced at both ends of the cable to ensure that all the current fed to the inner conductor returns through the shield [15]. This is an ill assumption at very low frequencies if parallel ground paths are available, but in the present case the sensor side is floating and the problem does not exist. Then, the transmission line model is implemented with a simple LC-lumped-circuit model. It is combined with a unidirectional transfer impedance model from shield to the inner conductor. Unlike an earlier proposition [14], the transfer impedance circuit is implemented without frequency dependent sources with just a current (M_{ZTIx}) controlled current source (I_{ZTIx}), voltage (M_{ZTVx}) controlled voltage source (E_{ZTVx}), and the transfer impedance model with R_T and L_T. The two previous parts are then combined into a complete distributed element, which is multiplied to form the full coupled lumped-element transmission line model [16].

Simulation results in Fig. 7 show that, with the fresh cable, disturbance amplitude stays below the IC immunity limit, whereas, with the aged cable, there are three disturbance peaks that exceed the IC immunity limit between 40 and 200 MHz. Thus, it is shown that the cable shielding performance deterioration due to combined thermal and mechanical aging can have a detrimental effect on the system performance during BCI test. This also means that the system can be susceptible to radiated disturbances during its intended use.

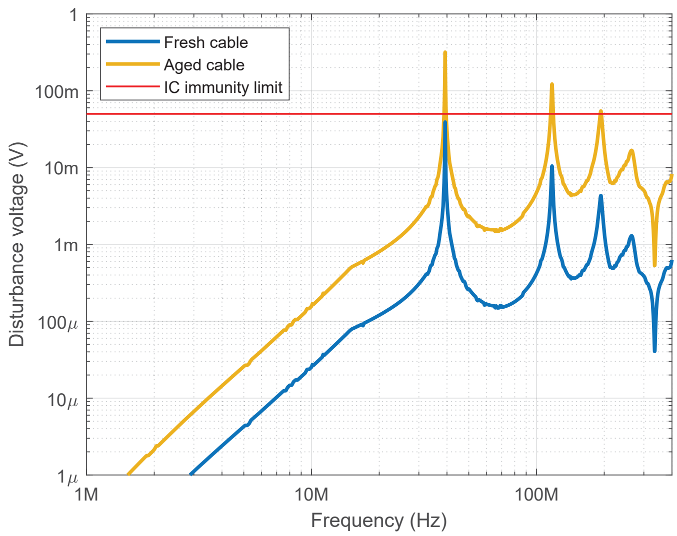

Fig. 7. BCI test simulation results at ECU IC input pin

V. Conclusion

In this paper, a method for thermal and mechanical aging of shielded cables, with the help of a triaxial cell specifically designed for environmental testing, was presented. To provide aging test results in reasonable time, highly accelerated life testing was used. It was demonstrated that the transfer impedance of a coaxial shielded cable with a combined foil and braid shield could suffer from significant aging. At low frequencies, the aging effect on transfer resistance is limited, but it seems that with a certain configuration of combined foil and braid shield, it is possible to observe a second lower level of transfer resistance, and this second level is susceptible to aging stresses. In addition, it was shown that the transfer inductance could increase by more than a decade during aging, which will have high consequences for system level immunity.

As the consequences to system level performance can be verified with a simulation model, it is possible to anticipate product performance already at concept level design. This gives the designers more possibilities to design for proper countermeasures for the aging effects.

The next step would be to do a thorough analysis on the reasons of shielding performance deterioration in this case and a comparison of different cable shield constructions. It is likely that performance reduction is related to deterioration of the foil part of the shield. Moreover, developing a triaxial test cell for environmental testing is not a straightforward task. There are specific trade-offs that are needed to achieve a good balance between mechanical and RF performances. These trade-offs necessitate further analysis.

ACKNOWLEDGMENT

The research leading to these results has received funding from the European Union's Horizon 2020 research and innovation programme under the Marie Skłodowska-Curie grant agreement No 812.790 (MSCA-ETN PETER). This publication reflects only the authors' view, exempting the European Union from any liability. Project website: http://etn-peter.eu/.

Authors would like to thank the staff of KU Leuven Bruges Campus FMEC laboratory for the possibility of conducting HALT. Especially, authors thank Prof. Davy Pissoort and Dr. Tim Claeys for test organization and partial financing. The first author would like to thank Ph.D. student Pejman Memar of KU Leuven for lending his office desk during writing this paper.

REFERENCES

[1] "ISO 11452-4:2020, Road vehicles — Component test methods for electrical disturbances from narrowband radiated electromagnetic energy — Part 4: Harness excitation methods," 2020.

[2] E. Knowles and L. Olson, "Cable Shielding Effectiveness Testing," *IEEE Trans. Electromagn. Compat.*, vol. EMC-16, no. 1, pp. 16–23, Feb. 1974.

[3] B. Démoulin and L. Koné, "Shielded Cable Transfer Impedance Measurements High frequency range 100 MHz–1 GHz," *IEEE Electromagn. Compat. Mag.*, no. 228, pp. 42–50, 2011.

[4] ——, "Shielded Cable Transfer Impedance Measurements in the Microwave Range of 1 GHz to 10 GHz," *IEEE Electromagn. Compat. Mag.*, no. 229, pp. 52–61, 2011.

[5] "ISO 16750-4:2010, Road vehicles — Environmental conditions and testing for electrical and electronic equipment — Part 4: Climatic loads," 2010.

[6] "ISO 16750-3:2012, Road vehicles — Environmental conditions and testing for electrical and electronic equipment — Part 3: Mechanical loads," 2012.

[7] H. Liu, T. Claeys, D. Pissoort, and G. A. E. Vandenbosch, "Characterizing EMI-filters' Deviations caused by the Capacitors Ageing based on Complex Impedance Analysis," in *2020 Int. Symp. on Electromagn. Compat. - EMC EUROPE*. Rome, Italy: IEEE, Sep. 2020, pp. 1–5.

[8] S. V. Suraci, D. Fabiani, S. Roland, and X. Colin, "Multi scale aging assessment of low-voltage cables subjected to radio-chemical aging: Towards an electrical diagnostic technique," *Polymer Testing*, vol. 103, p. 107352, Nov. 2021.

[9] J. Verpoorte, H. Schippers, and J. L. Rotgerink, "Advanced models for the transfer impedance of metal braids in cable harnesses," in *2018 IEEE Int. Symp. Electromagn. Compat. 2018 IEEE Asia-Pacific Symp. Electromagn. Compat. (EMC/APEMC)*. Singapore: IEEE, May 2018, pp. 187–192.

[10] B. Vanlandschoot and L. Martens, "New method for measuring transfer impedance and transfer admittance of shields using a triaxial cell," *IEEE Trans. Electromagn. Compat.*, vol. 39, no. 2, pp. 180–185, May 1997.

[11] General Motors, "GMW8287 - Highly Accelerated Life Testing," Feb. 2002.

[12] IEC TS 62153-4-1, *Metallic Communication Cable Test Methods – Part 4-1: Electromagnetic Compatibility (EMC) – Introduction to Electromagnetic Screening Measurements*, 2014.

[13] F. Lafon, "Développement de techniques et de méthodologies pour la prise en compte des contraintes CEM dans la conception d'équipements du domaine automobile. : Etude de l'immunité, du composant à l'équipement [Techniques and methodologies development to take into account EMC constraints in Automotive equipment design - Immunity analysis from component until the equipment]," Ph.D. dissertation, INSA Rennes, Rennes, France, Jan. 2011.

[14] G. Antonini, A. Scogna, A. Orlandi, and R. Rizzi, "Experimental validation of circuit models for bulk current injection (BCI) test on shielded coaxial cables," in *2004 Int. Symp. on Electromagn. Compat. (IEEE Cat. No.04CH37559)*, vol. 1. Silicon Valley, CA, USA: IEEE, 2004, pp. 63–68.

[15] M. Raya and R. Vick, "Network Model of Shielded Cables for the Analysis of Conducted Immunity and Emissions," *IEEE Trans. Electromagn. Compat.*, vol. 61, no. 4, pp. 1167–1174, Aug. 2019.

[16] T. Dhaene and D. de Zutter, "Selection of lumped element models for coupled lossy transmission lines," *IEEE Trans. Comput.-Aided Des. Integr. Circuits Syst.*, vol. 11, no. 7, pp. 805–815, Jul. 1992.